CoA. Report Aero. No. 167

THE COLLEGE OF AERONAUTICS

CRANFIELD

OPTIMUM MICHELL FRAMEWORKS FOR THREE PARALLEL FORCES

by

H.S.Y. Chan

REPORT AERO NO. 167

August, 1963

THE COLLEGE OF AERONAUTICS

CRANFIELD

Optimum Michell Frameworks for Three Parallel Forces

- by -

H.S.Y. Chan, B.A.

SUMMARY

The design of Michell optimum structures to carry three coplanar forces has been the most popular topic in this field. However, the mathematical technique involved so far has been rather limited in as much as only strictly symmetrical cases have been considered. It is the intention of the present paper to apply the general theory of optimum design to a rather complicated problem of this type, and study in full detail the outcoming mathematical concepts, both numerical and theoretical.

CONTENTS

1. Introduction

The fundamental problem of structural design is the determination of structures of minimum weight which safely equilibrate a given system of external forces. In the study of two-dimensional optimum Michell structures, it is of some advantage to make use of the analogy with the theory of plane plastic flow, which states that the members of a Michell frame lie along lines which have the same form as the slip lines in the plastic case. Several cases of practical interest were studied in great detail by A.S.L. Chan[2] using this method. The present work is concerned with the optimum design of a framework under a further case of three force loading, which is derived by an extension of the slip line field for one of the classical designs of Michell.

2. Geometrical layout

Consider the loading problem of Figure 1. The points of application of the forces lie on a straight line, with OP< PO′. The forces are all perpendicular to the line OO′ and in equilibrium. The problem is to construct a Michell structure which equilibrates these forces.

It is already known[1] that when OP = PO′, the optimum structure is as shown in Figure 2. The corresponding slip line field is presented in Figure 3, which shows that the slip lines in the region ACPA′C′ consist of circular arcs and radii, with AC′ perpendicular to A′C, whereas the slip lines in the squares OAPA′, O′CPC′ are merely orthogonal straight segments.

It is proposed to extend this slip line field outside its original region. The procedure is explained below, and is illustrated in Figures 4 and 5, because of the symmetry, it is sufficient to consider only the region above OO′.

(2.1) Beginning with Figure 1, determine first a point E on PO′, so that OP = PE. Then draw from O, P, E, the slip line fields OAP, APC and CPE, identical with those shown in Figure 3.

(2.2) Since the point O is a point of application of force, it is possible that it is a singular point similar to the point P. This suggests the introduction of a region OAB similar to APC.

(2.3) Two orthogonal arcs AB and AC, are now given, and so the slip line field can be extended to the whole region BACD in the manner of Figure 16 of Reference 2.

(2.4) The straight segment CE is perpendicular to CD, so the slip line field can now be extended to the whole region DCEF. Here, one set of the slip lines are straight segments which envelope an 'evolute'; the other set of slip lines are then 'involutes'. (see Reference 2, p. 5).

Up to now, the extensions of the slip line fields on either side of OO′ are separate from one another. Similar fields under the line OO′ are also shown in Figure 5. At this stage, they must, if possible, be brought together to complete the final layout.

(2.5) EF and EF′, are two orthogonal slip lines symmetrical with respect to OO′, so a slip line field can be obtained from them, each curve of which will intersect OO' at 45^{o}.

The layout of the required structure may now be obtained from the slip line field of Figure 5. The necessary structure for the proposed problem is given in Figure 4.

So far, no explanation has been given as to the method of constructing the layout analytically. As would be expected for such a complicated case, numerical solution of the analytical equations will become unavoidable. However, with the powerful graphical method developed in the theory of plasticity - see for instance Reference 3, Chapter 6 - one can obtain such a layout with sufficient degree of accuracy. The slip line field in Figure 5 was constructed by this graphical method with an increment of 10^{o} between adjacent slip lines.

3. Calculation of the virtual displacements

For the sake of convenience, some basic formulae are stated and notations explained, using Figure 6.*

The layout lines for the structure can be taken separately in each region as co-ordinate curves of a curvilinear co-ordinate system (α, β).

Denote $$\phi = -\alpha + \beta \tag{1}$$

which is the angle between the positive α-direction and the x-axis. The radii of curvature of the α, β curves are denoted by A and B respectively. They are related by

$$\frac{\partial A}{\partial \beta} = B \quad , \quad \frac{\partial B}{\partial \alpha} = A \tag{2}$$

The virtual displacements along the α, β curves are denoted by u and v. They satisfy the following expressions

$$\begin{cases} \dfrac{\partial u}{\partial \alpha} + v = -Ae \quad , & \dfrac{\partial u}{\partial \beta} - v = -B\omega \\ \dfrac{\partial v}{\partial \alpha} - u = A\omega \quad , & \dfrac{\partial V}{\partial \beta} + u = Be \end{cases} \tag{3}$$

where $$\omega(\alpha, \beta) = 2e(\alpha + \beta) + \omega(o.o) \tag{4}$$

is the rotation at any point (α, β) within the region, and $\pm e$ denote the principal strains. In what follows, the (α, β) co-ordinate systems are so chosen that the direct strain in the α-direction is always -e, and that in the β-direction is always +e, (see Figure 7).

(3.1) Start from region OAB, assuming, the origin O to be fixed. Since the (α, β) co-ordinates coincide with polar co-ordinates, the virtual displacements satisfy the following relations.

---

* Most of the notations used here are identical with those in Ref. 2.

$$\frac{\partial u}{\partial \alpha} = -e \quad , \quad \frac{\partial V}{\alpha \partial \beta} + \frac{u}{\alpha} = e \quad , \quad \frac{\partial V}{\partial \alpha} + \frac{\partial u}{\alpha \partial \beta} - \frac{v}{\alpha} = O \qquad (5)$$

and $u(o, o) = o = v(o, o)$.

The solution is
$$\begin{aligned} u(\alpha, \beta) &= -e\alpha \\ v(\alpha, \beta) &= 2e\alpha\beta + k\alpha \end{aligned} \qquad (6)$$

where k is a constant.

(3.2) Consider next the region OAP, and take the point A as origin. The (α, β) co-ordinates are simply Cartesian co-ordinates, and so

$$\frac{\partial u}{\partial \alpha} = -e \quad , \quad \frac{\partial v}{\partial \beta} = e \quad , \quad \frac{\partial u}{\partial \beta} + \frac{\partial v}{\partial \alpha} = O \qquad (7)$$

Deriving the boundary condition on OA from (6), one obtains the following result.

$$\begin{cases} u(\alpha, \beta) = -e\alpha + er - k\beta \\ v(\alpha, \beta) = e\beta + k\alpha - kr \end{cases} \qquad (8)$$

As
$$\begin{cases} u(P) = u(o, r) = r(e - k) \\ v(P) = v(o. r) = r(e - k) \end{cases} , \qquad (9)$$

the constant k is best chosen so that the point P is at rest, since this simplifies the remaining calculations considerably.

(3.3) In regions APC and CPE, the layout is the same as in (3.1) and (3.2). There is no need, therefore, to go into the same detail. After simple calculation, the following results are obtained.

On AB: $u = -er \quad , \quad v = er(2\beta + 1) \quad , \quad \omega(A) = e$ (10)

AC: $u = -er\,(2\alpha + 1) \quad , \quad v = er$ (11)

CE: $u = -e\alpha - er\,(1 + \pi) \quad , \quad v = e\alpha\,(1+\pi) + er$ (12)

where u, v and α, β in the above equations are consistant with the notations for the virtual displacements and co-ordinates used in regions BACD and DCEF, with points A and C respectively taken as origins, (see Figure 7).

At this stage, the classical solution of the structure in Figure 2 is already determined. From (12), the virtual displacements of the point E (which corresponds to point O′ in Figure 2) are

$$u = -er\,(2 + \pi) \quad , \quad v = er(2 + \pi) \qquad (13)$$

The resultant vertical displacement is

$$\sqrt{u^2 + v^2} = \sqrt{2}\,(2 + \pi)\,er = (2 + \pi)\,ed \quad ,$$

and so the volume V of the structure is

$$V = (2+\pi)\,d\,.\,\frac{F}{2f} = (1+\frac{\pi}{2})\,\frac{Fd}{f} \tag{14}$$

where f is the allowable stress in the members of the structure.

(3.4) For region BACD, the complete analysis had been carried out already in Reference 2, and the results are as follows.

$$\omega = 2e(\alpha+\beta) + \omega(A) = 2e(\alpha+\beta) + e \tag{15}$$

$$\left\{\begin{aligned} A(\alpha,\beta) &= r\left[I_o(2\sqrt{\alpha\beta}) + \sqrt{\frac{\beta}{\alpha}}\; I_1(2\sqrt{\alpha\beta})\right] \\ B(\alpha,\beta) &= r\left[I_o(2\sqrt{\alpha\beta}) + \sqrt{\frac{\alpha}{\beta}}\; I_1(2\sqrt{\alpha\beta})\right]\end{aligned}\right. \tag{16*}$$

$$\left\{\begin{aligned} u(\alpha,\beta) &= -er\left[(1+2\alpha)\,I_o(2\sqrt{\alpha\beta}) + 2\sqrt{\alpha\beta}\;I_1(2\sqrt{\alpha\beta})\right] \\ v(\alpha,\beta) &= er\left[(1+2\beta)\,I_o(2\sqrt{\alpha\beta}) + 2\sqrt{\alpha\beta}\;I_1(2\sqrt{\alpha\beta})\right]\end{aligned}\right. \tag{17}$$

The boundary conditions on CD can be obtained by setting $\alpha = \frac{\pi}{2}$, $\beta = 0$.

(3.5) In region DCEF, the (α, β) co-ordinates are shown in Figure 7. By Hencky's theorem[3], the variable β is identical with that in region BACD on corresponding α-lines. Since one set of slip lines are straight segments, the calculation of the layout is quite straight forward, taking into account the boundary conditions on CD, (Reference 2, § 4, case 2). The results are

$$A(\alpha,\beta) = 1 \quad , \quad B(\alpha,\beta) = \alpha + B(o,\beta) = \alpha + r\left[I_o(\sqrt{2\pi\beta}) + \sqrt{\frac{\pi}{2\beta}}\; I_1(\sqrt{2\pi\beta})\right] \tag{18}$$

$$\omega = 2e\beta + \omega(C) = e(2\beta + 1 + \pi) \tag{19}$$

$$\begin{aligned} u(\alpha,\beta) &= -e\alpha + u(o,\beta) = -e\alpha - er\left[(1+\pi)\,I_o(\sqrt{2\pi\beta}) + \sqrt{2\pi\beta}\;I_1(\sqrt{2\pi\beta})\right] \\ v(\alpha,\beta) &= \alpha\omega + v(o,\beta) = (2\beta+1+\pi)\,er + er\left[(1+2\beta)\,I_o(\sqrt{2\pi\beta}) + \sqrt{2\pi\beta}\;I_1(\sqrt{2\pi\beta})\right]\end{aligned} \tag{20}$$

(3.6) Finally, in region FEF', the (α, β) co-ordinates are shown also in Figure 7. By Hencky's theorem, the variable β is still identical with that of the previous case for corresponding α-lines. From (18), the radius of curvature B of this new co-ordinate system satisfies

$$B(o,\beta) = r\left[1 + I_o(\sqrt{2\pi\beta}) + \sqrt{\frac{\pi}{2\beta}}\; I_1(\sqrt{2\pi\beta})\right] \tag{21}$$

---

* $I_k(Z)$ denotes the modified Bessel function of the k^{-th} order, $I_k(Z) = i^{-k} J_k(iZ)$.

Because of symmetry, $A(\alpha, \beta) = B(\beta, \alpha)$, (22)

and so $A(\alpha, o) = B(o, \alpha) = r\left[1 + I_o(\sqrt{2\pi\alpha}) + \sqrt{\frac{\pi}{2\alpha}}\, I_1(\sqrt{2\pi\alpha})\right]$ (23)

From (19), $\omega = 2e(\alpha + \beta) + \omega(E) = 2e(\alpha + \beta) + e(1 + \pi)$ (24)

Using equation (2) and the boundary conditions (21), (23), A, and B can be obtained from the following formula (Reference 2, equation (27):

$$A(\alpha, \beta) = A(o,o)\, I_o(2\sqrt{\alpha\beta}) + \int_o^{\alpha} I_o(2\sqrt{(\alpha - \xi)\beta})\, \frac{\partial A(\xi, o)}{\partial \xi}\, d\xi + $$

$$+ \int_o^{\beta} I_o(2\sqrt{\alpha(\beta - \eta)})\, B(o, \eta)\, d\eta \qquad (25)$$

Details of this integration are presented in Appendix A, and the result gives, from (A.4), (A.10),

$$A(\alpha, \beta) = r\Bigg\{ (2 + \frac{\pi}{2})\, I_o(2\sqrt{\alpha\beta}) + \sqrt{\frac{\beta}{\alpha}}\, I_1(2\sqrt{\alpha\beta}) + \sqrt{\frac{2\beta}{2\alpha + \pi}}\, I_1(\sqrt{2\beta(2\alpha + \pi)}) + $$

$$+ \sum_{k=o}^{\infty} \frac{(-1)^k}{(k+1)!} \cdot \left(\frac{\pi}{2}\right)^{1+k} \cdot \left(\frac{2\alpha}{2\beta + \pi}\right)^{(1+k)/2} \cdot I_{1+k}(\sqrt{2\alpha(2\beta + \pi)}) + $$

$$+ \sum_{k=o}^{\infty} \frac{(-1)^k}{(k+1)!} \cdot \left(\frac{\pi}{2}\right)^{1+k} \cdot \left(\frac{2\beta}{2\alpha + \pi}\right)^{(1+k)/2} \cdot I_{1+k}(\sqrt{2\beta(2\alpha + \pi)}) + $$

$$+ \sum_{k=o}^{\infty} \frac{(-1)^k}{k!\,(k+2)} \cdot \left(\frac{\pi}{2}\right)^{2+k} \cdot \left(\frac{2\alpha}{2\beta + \pi}\right)^{(1+k)/2} \cdot I_{1+k}(\sqrt{2\alpha(2\beta + \pi)}) \Bigg\} \qquad (26)$$

The formulea for the virtual displacements are obtained by adding equation (3) in pairs

$$\left\{ \begin{aligned} \frac{\partial u}{\partial \alpha} + \frac{\partial u}{\partial \beta} &= -Ae - Be\,(2\alpha + 2\beta + 1 + \pi) \\ \frac{\partial v}{\partial \alpha} + \frac{\partial v}{\partial \beta} &= Be + Ae\,(2\alpha + 2\beta + 1 + \pi) \end{aligned} \right. \qquad (27)$$

Letting $\sigma = \alpha + \beta$, $\tau = \alpha - \beta$, (27) becomes

$$\begin{aligned} 2\frac{\partial u}{\partial \sigma} &= -Ae - Be\,(2\sigma + 1 + \pi) \\ 2\frac{\partial v}{\partial \sigma} &= Be + Ae\,(2\sigma + 1 + \pi) \end{aligned} \qquad (28)$$

Theoretically speaking, once the values of u and v on the boundary are known, this set of equations can be integrated along the line τ = constant to obtain $u(\alpha, \beta)$ and $v(\alpha, \beta)$. Owing to the complexity of equation (26), it does not seem possible to obtain an analytical expression for u, v. However, for the solution of the present problem, it is of interest to calculate only those values of u, v on the line $\tau = o$.

Letting $\alpha = \frac{\sigma}{2} = \beta$ in (28) and noticing (22), the following integral expression is derived,

$$u(\mu, \mu) = u(E) - \frac{e}{2} \int_{o}^{2\mu} (2\sigma + 2 + \pi) A\left(\frac{\sigma}{2}, \frac{\sigma}{2}\right) d\sigma$$

$$= -(2+\pi) er - e \int_{o}^{1} \mu (4\mu t + 2 + \pi) A(\mu t, \mu t) \, dt, \qquad (29)$$

where

$$A(\mu t, \mu t) = r\left\{ \left(2 + \frac{\pi}{2}\right) I_o(2\mu t) + I_1(2\mu t) + \sqrt{\frac{2\mu t}{2\mu t + \pi}}\, I_1\left(\sqrt{2\mu t(2\mu t + \pi)}\right) + \right.$$

$$\left. + \sum_{k=o}^{\infty} \frac{(-1)^k}{k!} \left[\frac{2}{k+1} + \frac{\pi}{2k+4} \right] \cdot \left(\frac{\pi}{2}\right)^{1+k} \cdot \left(\frac{2\mu t}{2\mu t + \pi}\right)^{(1+k)/2} \cdot I_{1+k}\left(\sqrt{2\mu t(2\mu t + \pi)}\right) \right\}$$

(30)

Finally, by symmetry, $v(\mu, \mu) = -u(\mu, \mu)$ (31)

Detailed consideration of the numerical calculations is given in Appendix B. The results are shown in Table 1.

4. Volume of the Michell structures

Before calculating the volume of the structures, it is necessary to relate the (α, β) co-ordinates to distances along OPO'.

Referring to the co-ordinate system in region FEF', the direction cosines of the tangent lines to the co-ordinate curves are given by, (Reference 2, equation (22)),

$$\cos\phi = \frac{1}{A}\frac{\partial x}{\partial \alpha} = \frac{1}{B}\frac{\partial y}{\partial \beta}$$
$$\sin\phi = \frac{1}{A}\frac{\partial y}{\partial \alpha} = \frac{-1}{B}\frac{\partial x}{\partial \beta} \qquad (32)$$

where ϕ is defined by (1). This equation (32) gives

$$x = \int^{(\alpha,\beta)} (A \cos \phi \, d\alpha - B \sin \phi \, d\beta)$$
$$y = \int^{(\alpha,\beta)} (A \sin \phi \, d\alpha + B \cos \phi \, d\beta) \tag{33}$$

which takes a rather simple form when integrated along the line EO′. For any point O′(α, β) on EO′, the following relations are satisfied.

$$\begin{cases} \alpha = \mu = \beta \\ \cos \phi = 1, \quad \sin \phi = 0 \\ A(\mu, \mu) = B(\mu, \mu) \end{cases} \tag{34}$$

Substituting (34) into (33) gives

$$x = \int_0^{\mu} A(\alpha, \alpha) d\alpha = \int_0^{\mu} B(\beta, \beta) d\beta = y \tag{35}$$

The integral

$$x = \int_0^{\mu} A(\alpha, \alpha) d\alpha = \int_0^{1} A(\mu t, \mu t)\, dt \tag{36}$$

can be calculated in exactly the same way as that of equation (29). Referring to Figure 7, the final relation is

$$\ell - d = EO' = \sqrt{x^2 + y^2} = \sqrt{2}x \tag{37}$$

Notice that the angle μ must be less than 135°, otherwise the slip line fields at point O will overlap. This shows that the length, ℓ, will attain an upper limit when $\mu = 135^{\circ}$. A curve is plotted in Figure 8, showing this relationship, and the corresponding numerical results are shown in Table 1.

Another but less accurate way of obtaining the relation between ℓ/d and μ is to measure the graphical layout of Figure 5, for several values of μ. With the help of interpolation, the relation at any position of EO′ can be found.

The volume of the structures can now be determined. Assuming O, P, O′, are the points of action of the forces, then, referring to Figure 1 once more,

$$F_2 = \frac{d}{d+\ell} F \tag{38}$$

The resultant displacement of the point O′ is, from (29), (31), along the line of action of the force F_2 and its magnitude is equal to $-\sqrt{2}u(\mu, \mu)$. Since the points O and P are at rest, the volume of the required structure is

$$V = -\sqrt{2}\, u(\mu, \mu) \frac{F_2}{ef} = \frac{-\sqrt{2}d}{d+\ell}\, u(\mu, \mu) \frac{F}{ef} \tag{39}$$

The numerical results are shown also in Table 1. A curve is plotted in Figure 9 indicating the complete set of solutions.

An approximate estimate of the volume required may be obtained from Figure 10. This has been constructed using the graphical method, (Reference 2, § 6), and from this, the loads carried by each member can be calculated by statical analysis starting from point O'. The length of each member can be obtained by measurement. This gives an approximate solution for the required structure. An example of such a calculation is recorded by the numbers attached on each member of Figure 10. Some values are tabulated below for a direct comparison with the theoretical results.

ℓ/d	$\frac{Vf}{Fd}$ (eq. (39))	$\frac{Vf}{Fd}$ (graphical solution)
1	2.5708	-
1.5	3.1366	3.269
2	3.5896	3.63
2.5	3.9662	4.082
3	4.2882	4.398
3.5	4.5702	4.68
4	4.8210	4.938
4.5	5.0462	5.182
5	5.2495	5.402

5. The limiting case for ℓ/d large.

It is shown in Table 1 that the solutions exist only for those cases satisfying

$$1 \leqslant \frac{\ell}{d} < 149.1764 \tag{40}$$

If this relation does not hold, OP becomes very small in comparison with PO', and $F_1 \gg F_2$ It is then natural to approximate the loadings at O and P by a force F^* per unit length continuously distributed on the circumference of a circle Q, with OP as diameter and center Q lying midway between O and P, (see Figure 11), such that the resultant is a vertical force F_2 and a moment $F_2 \cdot (\frac{d}{2} + \ell)$ at Q.

Such a loading problem is known as Michell's Cantilever (Reference 1, ex. 1), the slip line field of which consists of equiangular spirals. If polar co-ordinates (ρ, θ) are introduced at center Q, the spirals have the form, (Reference 4, (3.15)),

$$\begin{aligned} &\alpha \text{ - curves} \qquad \rho = ke^{\theta - 2\beta + \frac{\pi}{4}} \\ &\beta \text{ - curves} \qquad \rho = ke^{-\theta + 2\alpha - \frac{\pi}{4}}, \end{aligned} \qquad k > o \text{ is a constant} \tag{41}$$

which shows that the co-ordinate curves

$$\rho = \text{const.} \quad \text{and} \quad \theta = \text{const.}$$

are lines of principal strain, (represented by dotted lines in Figure 12). If u, v are virtual displacements along ρ and θ directions, then

$$\left\{ \begin{array}{l} \frac{\partial u}{\partial \rho} = 0 \ , \quad \frac{\partial v}{\rho \partial \theta} + \frac{u}{\rho} = 0 \\ \frac{\partial u}{\rho \partial \theta} + \frac{\partial v}{\partial \rho} - \frac{v}{\rho} = 2e \ , \end{array} \right. \tag{42}$$

(e is the allowable strain), which gives

$$\begin{aligned} u &= C_1 \sin\theta - C_2 \cos\theta \\ v &= C_2 \sin\theta + C_1 \cos\theta + C_3 \rho + 2e\rho \ln\rho \end{aligned} \tag{43}$$

where C_1, C_2, C_3, are constants of integration. Assuming the point Q to be fixed, then $C_1 = C_2 = 0$. The third constant can be chosen to bring the point O′ to rest, that is

$$C_3 = -2e \ \ln\left(\ell + \frac{d}{2}\right) \tag{44}$$

The virtual displacements at the boundary of the circle Q are, by (43) and (44),

$$\left\{ \begin{array}{l} u = o \\ v = -\frac{d}{2} \cdot 2e \ln\left(1 + 2\frac{\ell}{d}\right) \end{array} \right. \tag{45}$$

The volume of the structure is then given by the work by F^*. The result is

$$\begin{aligned} efV &= \int_o^{2\pi} F^* \cdot \frac{d}{2} \cdot 2e \ln\left(1 + 2\frac{\ell}{d}\right) d\theta \\ &= 2e \ln\left(1 + 2\frac{\ell}{d}\right) \cdot \int_o^{2\pi} F^* \cdot \frac{d}{2} \, d\theta \\ &= 2e \ln\left(1 + 2\frac{\ell}{d}\right) \cdot F_2 \cdot \left(\frac{d}{2} + \ell\right) \end{aligned} \tag{46}$$

Finally, by using (38), the above expression can be put into a form similar to (39),

$$V = \left(2 - \frac{d}{\ell + d}\right) \cdot \ln\left(1 + 2\frac{\ell}{d}\right) \cdot \frac{Fd}{f} \tag{47}$$

The numerical values of (47) are plotted as a dotted line in Figure 9, which indicates the similarity of the two solutions. If the original loading problem of § 2 has been formulated in the manner used here, then equation (47) would give the required volume of structure. The layout of the Michell Cantilever can be extended to infinity, and this gives a more complete solution. The present solution, however, covers what may be expected to be a practical range of geometrical layouts.

A further remark may be made. If the point P is situated above OO′ and the angle OPO′ is greater than a right angle, a similar approach can be adopted. Michell's original structure for the case OP = PO′ and the corresponding extension of the slip line field are shown in Figures 13 and 14.

Acknowledgment

The author wishes to acknowledge the guidance given by Professor W.S. Hemp who first stimulated the author's interest in this subject and has provided invaluable suggestions for the completion of this paper.

References

1. Michell, A.G.M. — The limit of economy of material in frame structures. Phil. Mag. Series VI, Vol. 8, 1904, pp. 589-597

2. Chan, A.S.L. — The design of Michell optimum structures. College of Aeronautics Report 142, 1960.

3. Hill, R. — Mathematical Theory of Plasticity. Oxford, Clarendon Press, 1950.

4. Hemp, W.S. — Theory of structural design. College of Aeronautics Report 115, 1958.

5. C.I.T. — Tables of integral transforms, V.2. Bateman Manuscript Project. McGraw Hill, 1954.

6. Bailey, W.N. — On integrals involving Bessel functions. Quart. J. Math., Oxford Series, Vol. 9, 1938. pp. 141-147.

7. Watson, G.N. — Theory of Bessel Functions. Cambridge Univ. Press, 1944.

8. N.P.L. — Modern Computing Method. Notes on Applied Science, No. 16, 1961.

μ (degrees)	$\frac{u(\mu,\mu)}{(-er)}$ (eq. 29)	$\frac{\ell}{d}$ (eq. 37)	$\frac{Vf}{Fd}$ (eq. 39)
0	5.1416	1.0000	2.5708
5	6.9360	1.3372	2.9677
10	9.1725	1.7317	3.3578
15	11.9515	2.1934	3.7426
20	15.3953	2.7342	4.1228
25	19.6527	3.3681	4.4991
30	24.9043	4.1113	4.8724
35	31.3698	4.9832	5.2430
40	39.3156	6.0066	5.6112
45	49.0646	7.2082	5.9775
50	61.0086	8.6196	6.3421
55	75.6220	10.2780	6.7053
60	93.4789	12.2274	7.0671
65	115.2746	14.5193	7.4278
70	141.8499	17.2149	7.7876
75	174.2214	20.3862	8.1464
80	213.6173	24.1180	8.5046
85	261.5221	28.5105	8.8620
90	319.7278	33.6820	9.2188
95	390.3979	39.7721	9.5751
100	476.1433	46.9456	9.9309
105	580.1131	55.3969	10.2863
110	706.1051	65.3557	10.6412
115	858.6982	77.0934	10.9958
120	1043.4130	90.9303	11.3500
125	1266.8977	107.2448	11.7040
130	1537.1629	126.4841	12.0577
135	1863.8560	149.1764	12.4111

Table 1.

Appendix A

Integration of equation (25)

From equations (21) and (23), it is found that

$$\frac{\partial A(\xi\ ,o)}{\partial \xi} = r\left[\sqrt{\frac{\pi}{2\xi}}\ I_1(\sqrt{2\pi\xi}\ ) + \frac{\pi}{2\xi}\ I_2(\sqrt{2\ \pi\xi}\ )\right] \tag{A.1}$$

$$B(o,\eta\ ) = r\left[\ 1 + I_o(\sqrt{2\pi\eta}\ ) + \sqrt{\frac{\pi}{2\eta}}\ I_1(\sqrt{2\ \pi\ \eta}\ )\right] \tag{A.2}$$

and because

$$\lim_{Z\to o}\ Z^{-k}\ I_k(Z) = \frac{1}{2^k\ \Gamma\ (k+1)} \quad \text{for any } k > o, \tag{A.3}$$ *

therefore

$$A(o,o) = r(2+\frac{\pi}{2}) \tag{A.4}$$

Substituting from (A.1,2) in (25) :-

$$\int_o^{\alpha} I_o(2\sqrt{(\alpha-\xi)\beta})\ \frac{\partial A(\xi\ ,o)}{\partial\xi}\,d\xi \quad + \int_o^{\beta} I_o(2\sqrt{\alpha(\beta-\eta)}\ )\ B\ (o,\eta\ )d\eta$$

$$= r\int_o^{\alpha} I_o(2\sqrt{(\alpha-\xi)\beta})\left[\sqrt{\frac{\pi}{2\xi}}\ I_1(\sqrt{2\pi\xi}\ ) + \frac{\pi}{2\xi}\ I_2(\sqrt{2\pi\xi}\ )\right. \ d\xi$$

$$+\ r\int_o^{\beta} I_o(2\sqrt{\alpha(\beta-\eta)}\left[\ 1 + I_o(\sqrt{2\pi\eta}\ ) + \sqrt{\frac{\pi}{2\eta}}\ I_1(\sqrt{2\pi\eta}\ )\right]d\eta$$

Next, by substituting $\xi = \alpha\sin^2\zeta$, $\eta = \beta\ \sin^2\zeta$, the two integrals can be combined to give the following

$$A(\alpha\ ,\beta\ ) - A(o,o)\ I_o\ (2\sqrt{\alpha\beta}\ ) = 2r\int_o^{\frac{\pi}{2}} I_o(2\sqrt{\alpha\beta}\ \cos\zeta)\left[\sqrt{\frac{\pi\alpha}{2}}\ \frac{I_o(\sqrt{2\pi\alpha}\ \sin\zeta\ )}{\sin\zeta} + \right.$$

$$\left. + \frac{\pi}{2}\ \frac{I_2(\sqrt{2\pi\alpha}\ \sin\zeta\ )}{\sin^2\zeta} + \beta + \beta\, I_o(\sqrt{2\pi\beta}\ \sin\zeta\ ) + \sqrt{\frac{\pi\beta}{2}}\ \frac{I_1(\sqrt{2\pi\beta}\ \sin\zeta)}{\sin\zeta}\right]\sin\zeta\ \cos\zeta\ d\zeta \tag{A.5}$$

---

* This expression can be derived, for example, by taking limit in Sonine's first finite integral, see § 12.11 of Reference 7.

The integrands in (A.5) have the standard forms, for which the result of integration can be found, for instance, in References 5, 6, 7. They are

$$\int_0^{\frac{\pi}{2}} I_o(p \cos\zeta) \sin\zeta \cos\zeta \, d\zeta = \frac{1}{p^2} \int_0^p I_o(Z) Z \, dZ = \frac{I_1(p)}{p} \qquad (A.6)$$

$$\int_0^{\frac{\pi}{2}} I_o(p \cos\zeta) I_o(q \sin\zeta) \sin\zeta \cos\zeta \, d\zeta = \frac{I_1(\sqrt{p^2+q^2})}{\sqrt{p^2+q^2}} \qquad (A.7)$$

$$\int_0^{\frac{\pi}{2}} I_o(p \cos\zeta) I_1(q \sin\zeta) \cos\zeta \, d\zeta = \frac{1}{2} \sum_{k=o}^{\infty} \frac{(-1)^k}{2^k.(k+1)!} \cdot \frac{q^{1+2k}}{(p^2+q^2)^{1+k/2}} I_{1+k}(\sqrt{p^2+q^2}) \qquad (A.8)$$

$$\int_0^{\frac{\pi}{2}} I_o(p \cos\zeta) I_2(q \sin\zeta) \frac{\cos\zeta}{\sin\zeta} d\zeta = \frac{1}{4} \sum_{k=o}^{\infty} \frac{(-1)^k}{2^k k!(k+2)} \cdot \frac{q^{1+2k}}{(p^2+q^2)^{(1+k)/2}} I_{1+k}(\sqrt{p^2+q^2}) \qquad (A.9)$$

where p, q are independent of ζ.

Comparing these general formulae with equation (A.5), the final result is

$$\begin{aligned} A(\alpha,\beta) - A(o,o) I_o(2\sqrt{\alpha\beta}) = r \Bigg\{ & \frac{\sqrt{\beta}}{\sqrt{\alpha}} I_1(2\sqrt{\alpha\beta}) + \sqrt{\frac{2\beta}{2\alpha+\pi}} \cdot I_1(\sqrt{2\beta(2\alpha+\pi)}) \\ & + \sum_{k=o}^{\infty} \frac{(-1)^k}{(k+1)!} \cdot \left(\frac{\pi}{2}\right)^{1+k} \cdot \left(\frac{2\alpha}{2\beta+\pi}\right)^{(1+k)/2} \cdot I_{1+k}(\sqrt{2\alpha(2\beta+\pi)}) \\ & + \sum_{k=o}^{\infty} \frac{(-1)^k}{(k+1)!} \cdot \left(\frac{\pi}{2}\right)^{1+k} \cdot \left(\frac{2\beta}{2\alpha+\pi}\right)^{(1+k)/2} \cdot I_{1+k}(\sqrt{2\beta(2\alpha+\pi)}) \\ & + \sum_{k=o}^{\infty} \frac{(-1)^k}{k!(k+2)} \cdot \left(\frac{\pi}{2}\right)^{2+k} \cdot \left(\frac{2\alpha}{2\beta+\pi}\right)^{(1+k)/2} \cdot I_{1+k}(\sqrt{2\alpha(2\beta+\pi)}) \Bigg\} \end{aligned} \qquad (A.10)$$

Appendix B

Numerical analysis of equation (29)

Before applying any method of numerical integration, it is of some interest to examine the series

$$\sum_{k=o}^{\infty} a_k(\mu\, t) = \sum_{k=o}^{\infty} \frac{(-1)^k}{k!} \cdot \left[\frac{2}{k+1} + \frac{\pi}{2k+4}\right] \cdot \left(\frac{\pi}{2}\right)^{1+k} \cdot \left(\frac{2\mu\, t}{2\,\mu\, t+\pi}\right)^{(1+k)/2} \cdot I_{1+k}(\sqrt{2\,\mu t(2\mu t+\pi)}\,) \tag{B.1}$$

more carefully.

Making use of the following result, (see Reference 7, § 2.12)

$$|J_k(Z)| \leqslant \frac{|\frac{1}{2}Z|^k}{k!} \quad e^{\frac{1}{4}|Z|^2}, \quad \text{for } k \geqslant o, \tag{B.2}$$

the modulus of the k-th term of the series is

$$\begin{aligned} |a_k(\mu t)| &\leqslant \frac{(2+\frac{\pi}{2})}{(k+1)!} \cdot \left(\frac{\pi}{2}\right)^{1+k} \cdot \left(\frac{2\,\mu t}{2\,\mu t+\pi}\right)^{(1+k)/2} \cdot \; |J_{1+k}(\sqrt{2\,\mu t(2\,\mu\, t+\pi\,)}\,)| \\ &\leqslant \frac{(2+\frac{\pi}{2})}{(k+1)!} \cdot \left(\frac{\pi}{2}\right)^{1+k} \cdot \left(\frac{2\mu\, t}{2\,\mu t+\,\pi}\right)^{(1+k)/2} \cdot \frac{(\frac{1}{2}\sqrt{2\mu\, t(2\,\mu\, t+\,\pi)}\,)^{1+k}}{(k+1)!}\, e^{\frac{\mu t}{2}(2\mu\, t+\pi)} \\ &= (2+\frac{\pi}{2})\, e^{\frac{\mu t}{2}(2\,\mu t+\,\pi)} \cdot \frac{(\frac{\pi}{2}\mu t)^{1+k}}{[(k+1)!]^2} \end{aligned} \tag{B.3}$$

This shows that the series of (B.1) converges even faster than the exponential series, and integration term by term is therefore permissible. Furthermore, summing the series (B.1) from k = N shows, by using (B.3),

$$\begin{aligned} \sum_{k=N}^{\infty} a_k(\,\mu t) &< (2+\frac{\pi}{2})\, e^{\frac{\mu}{2}(2\mu+\pi\,)} \sum_{k=N}^{\infty} \frac{(\frac{\pi}{2}\,\mu\,)^{1+k}}{[(k+1)!\,]^2} \\ &< (2+\frac{\pi}{2})\, e^{\frac{\mu}{2}(2\mu+\pi)} \sum_{k=N}^{\infty} \frac{(\frac{\pi}{2}\,\mu\,)^{1+k}}{[(N+1)!\;(N+2)^{k-N}\,]^2} \\ &= (2+\frac{\pi}{2})\, e^{\frac{\mu}{2}(2\mu+\pi\,)} \cdot \frac{(\frac{\pi}{2}\,\mu\,)^{1+N}}{[(N+1)!]^2} \cdot \sum_{k=N}^{\infty} \left[\frac{\frac{\pi}{2}\,\mu}{(N+2)^2}\right]^{k-N} \\ &= (2+\frac{\pi}{2})\, e^{\frac{\mu}{2}(2\mu+\pi\,)} \cdot \frac{(\frac{\pi}{2}\mu\,)^{1+N}}{[(N+1)!\,]^2} \; \frac{1}{\left[1-\frac{\pi}{2}\mu\,/(N+2)^2\right]} \end{aligned} \tag{B.4}$$

provided that $(N+2)^2 > \frac{\pi}{2}\ \mu$. This result can be used to estimate the number of terms required in numerical calculations.

For the numerical integration of equation (29) (and (36)), Simpson's Rule is adopted, which is particularly suitable for automatic computing, (see for instance Reference 8). The detail of the numerical work can best be explained by the flow diagram of computing below. The result of computing shows that up to seven terms of the series (B.1) have been used, and the interval of integration [0.1] has been divided up into 128 equal parts.

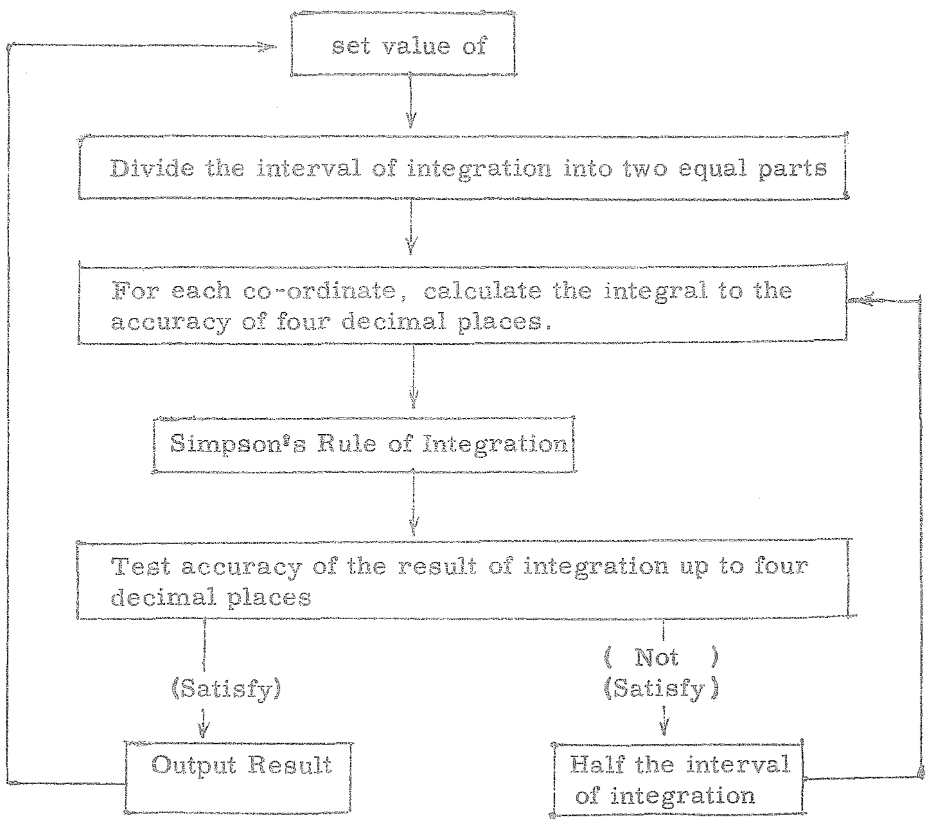

FIG. 1.

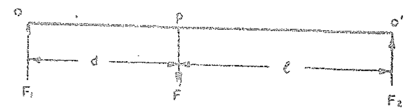

$d \leq \ell$

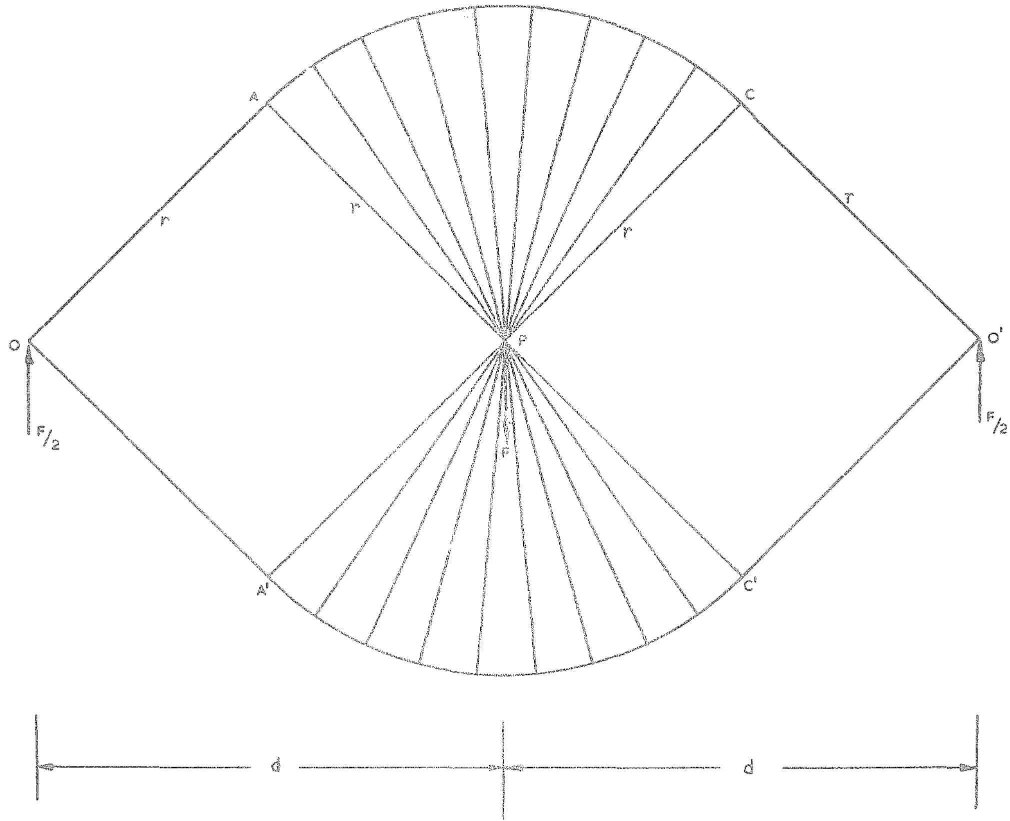

FIG. 2

$r = d/\sqrt{2}$

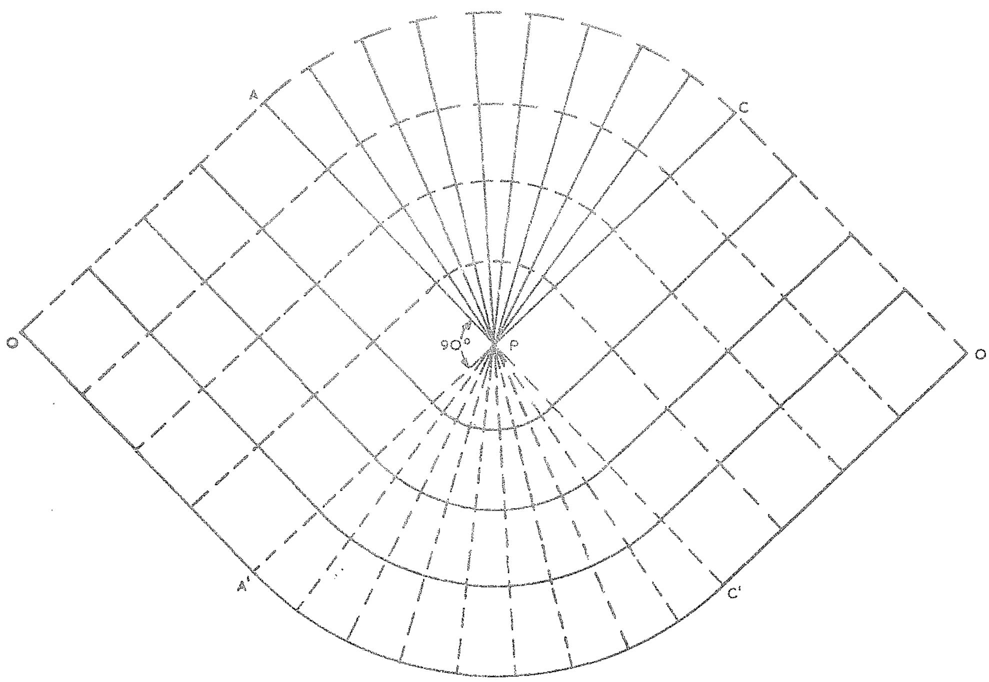

PRINCIPAL STRAIN $-e$

PRINCIPAL STRAIN $+e$

FIG. 3

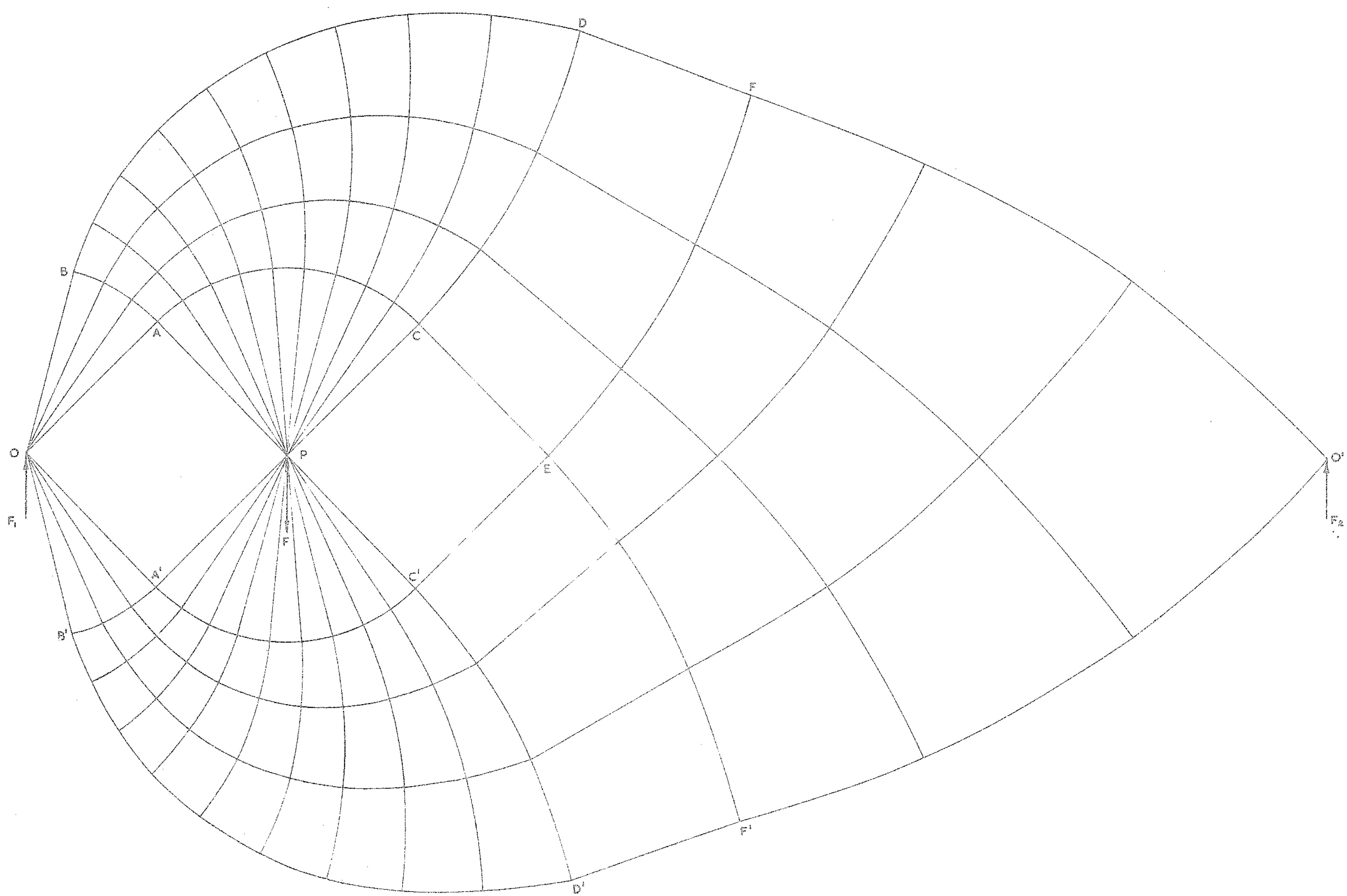

FIG. 4. OPTIMUM DESIGN FOR THREE PARALLEL FORCES

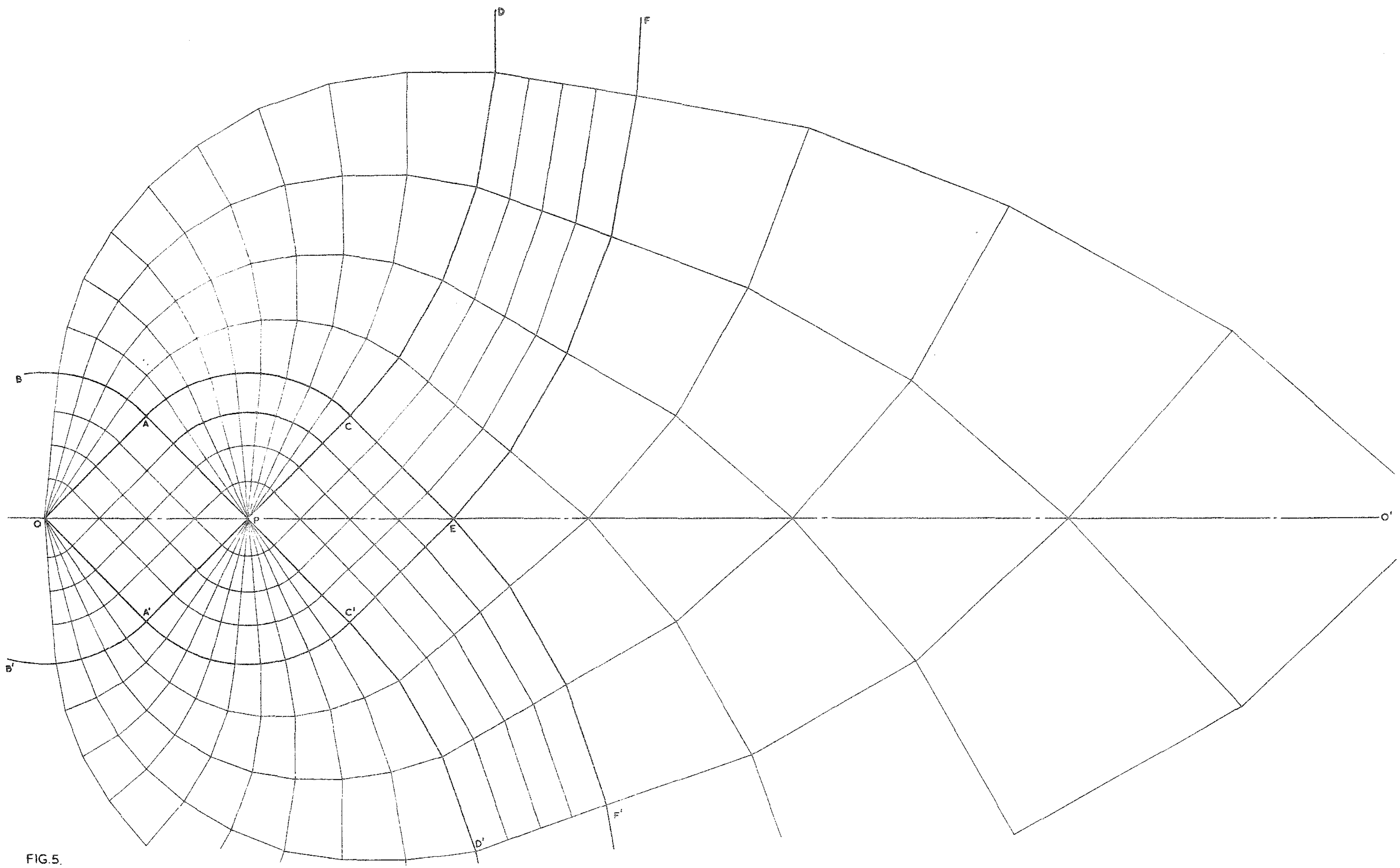

FIG.5.

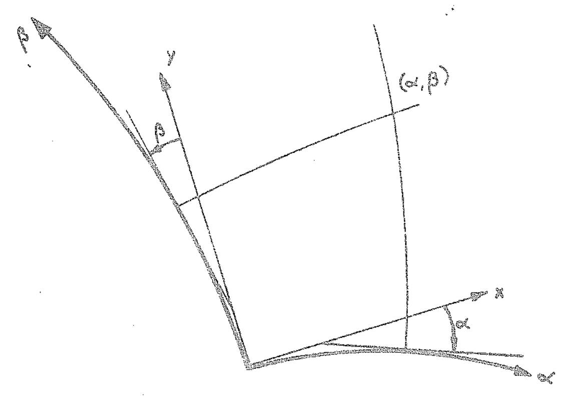

FIG. 6

$\phi = -\alpha + \beta$

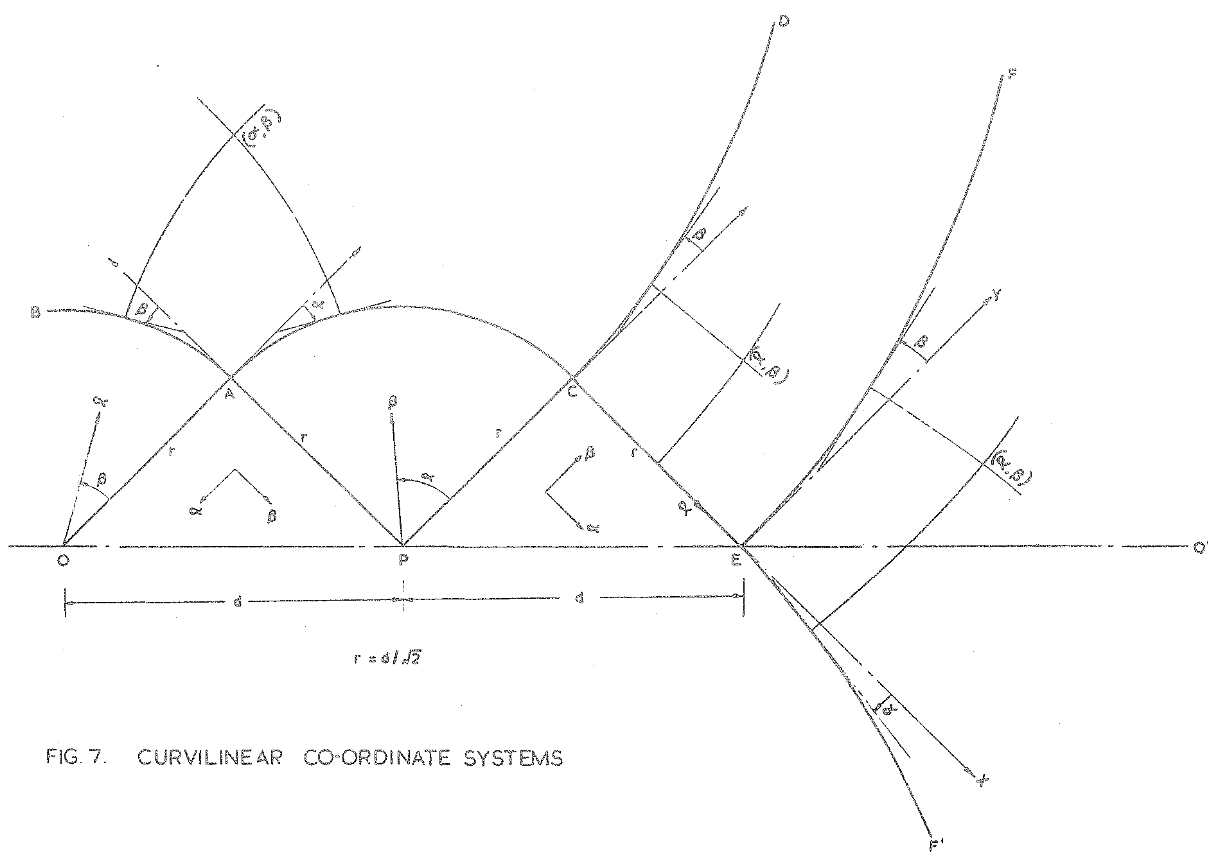

FIG. 7. CURVILINEAR CO-ORDINATE SYSTEMS

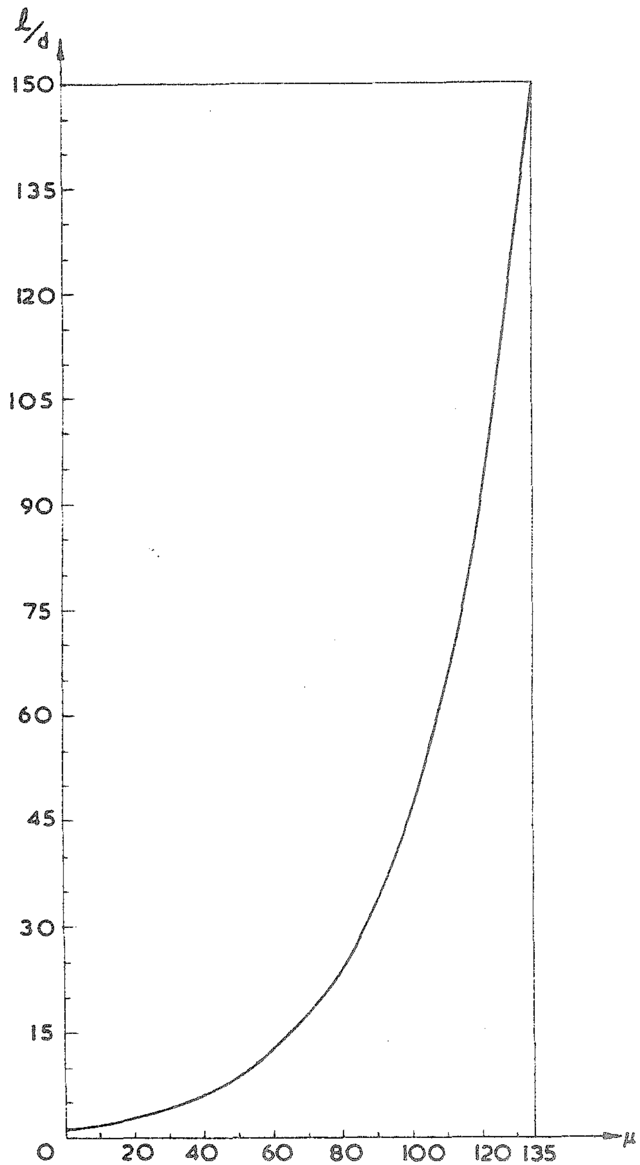
ℓ/d
150
135
120
105
90
75
60
45
30
15
0
20
40
60
80
100
120
135
μ

FIG. 8

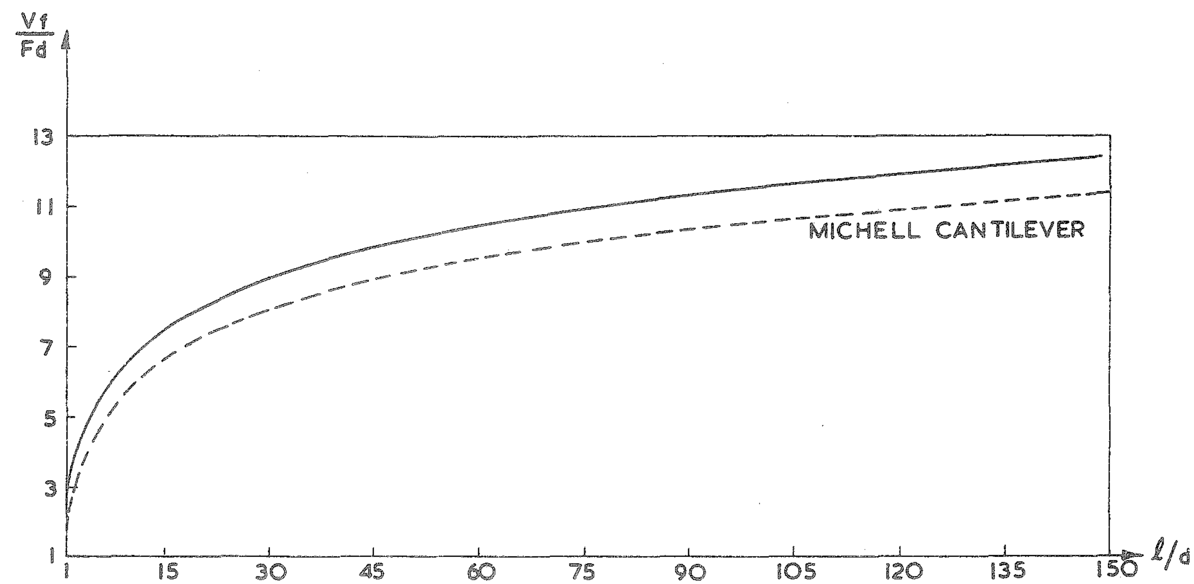
Vf/Fd
13
11
9
7
5
3
1
1
15
30
45
60
75
90
105
120
135
150
ℓ/d
MICHELL CANTILEVER

FIG. 9.

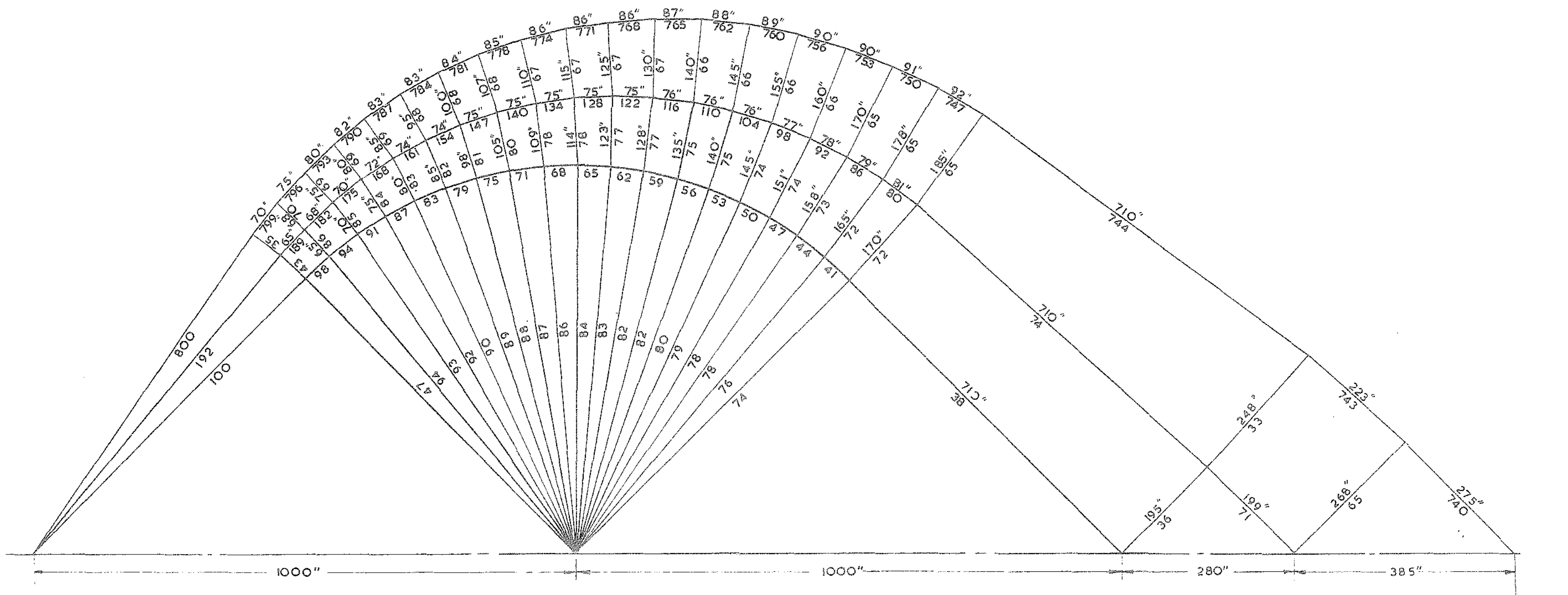

FIG. 10. (SCALE 1000" : 30 cm.)

FIG. II.

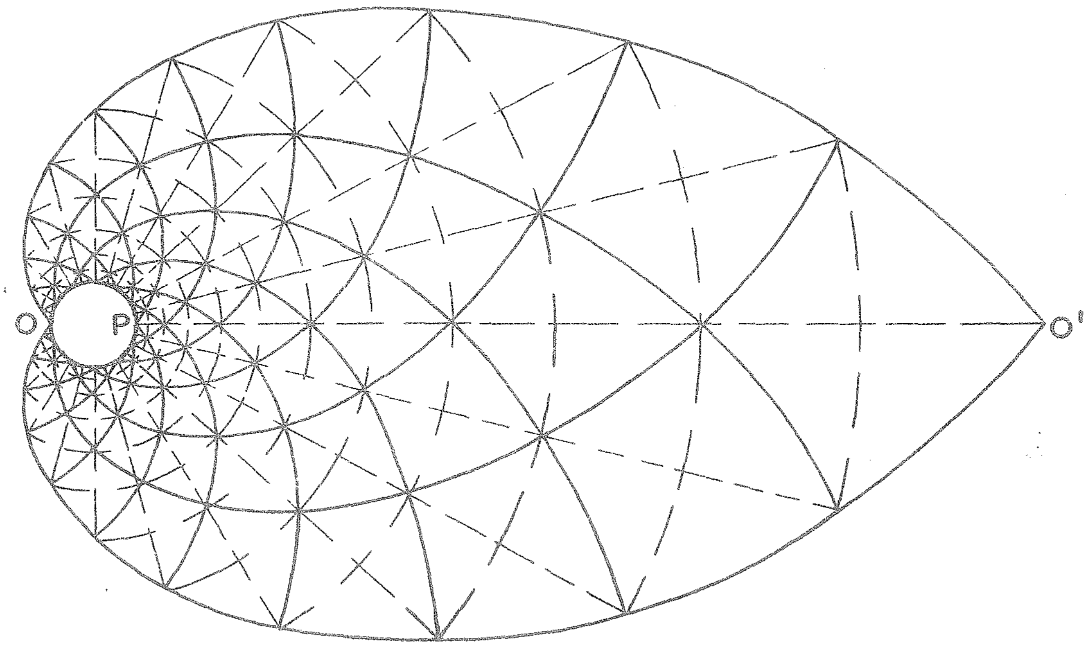

FIG. 12 MICHELL CANTILEVER

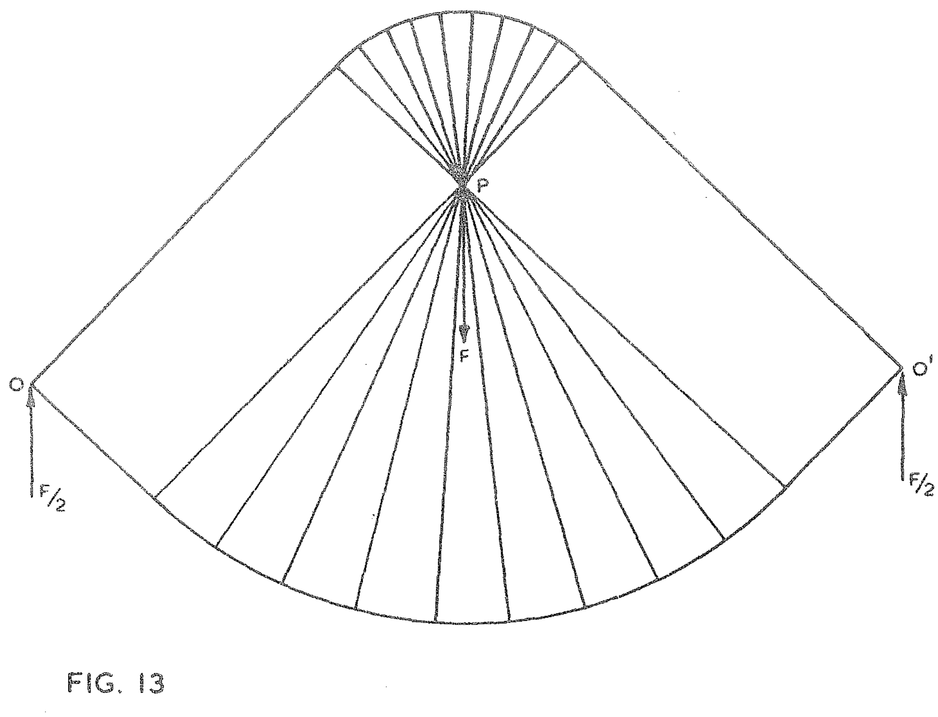

FIG. 13

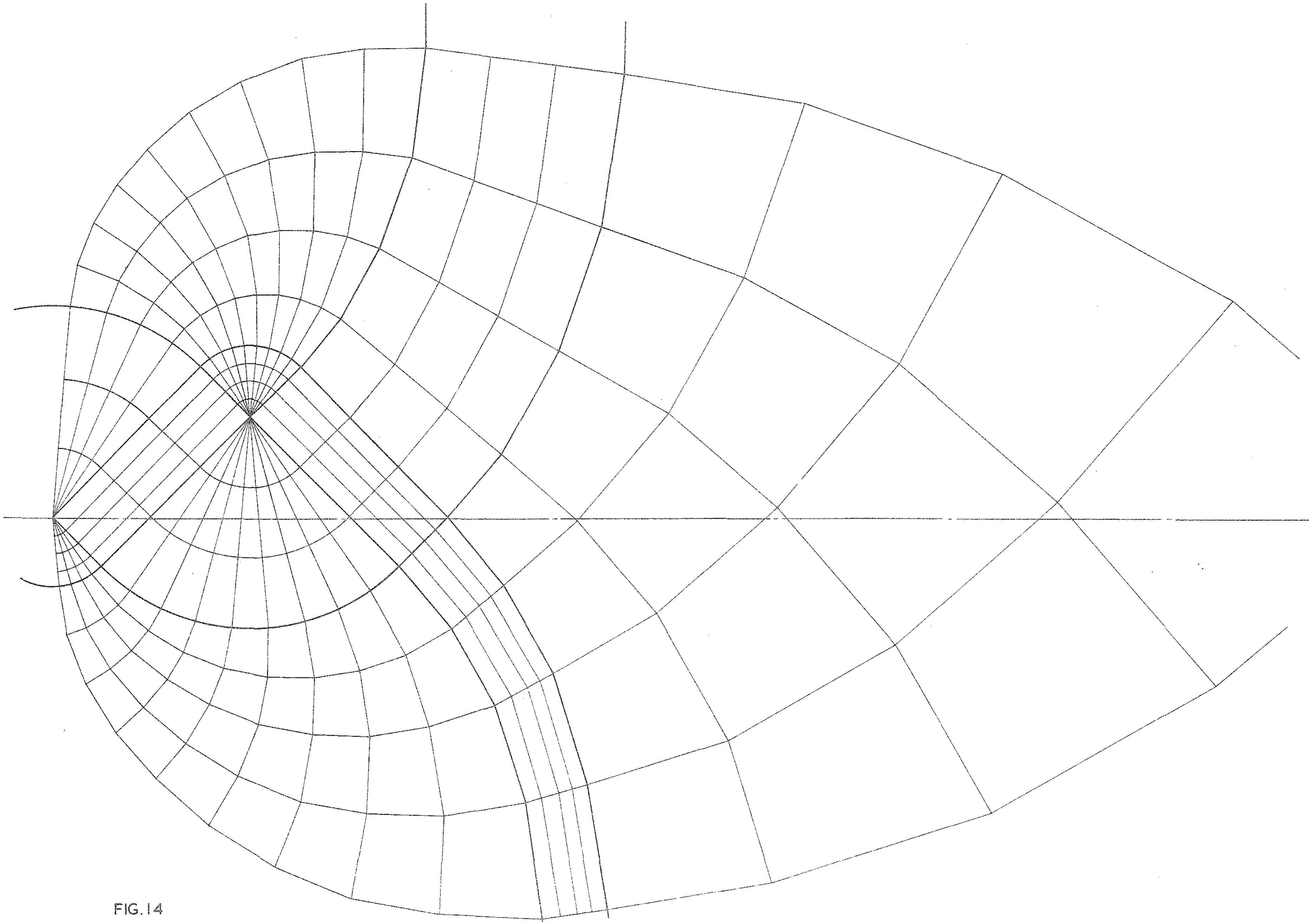

FIG. 14